

Observational constraints on dark energy with a fast varying equation of state

This article has been downloaded from IOPscience. Please scroll down to see the full text article.

JCAP05(2012)029

(<http://iopscience.iop.org/1475-7516/2012/05/029>)

View [the table of contents for this issue](#), or go to the [journal homepage](#) for more

Download details:

IP Address: 61.19.231.98

The article was downloaded on 25/05/2012 at 02:40

Please note that [terms and conditions apply](#).

Observational constraints on dark energy with a fast varying equation of state

Antonio De Felice,^{a,b} Savvas Nesseris^c and Shinji Tsujikawa^d

^aThEP's CRL, NEP, The Institute for Fundamental Study, Naresuan University, Phitsanulok 65000, Thailand

^bThailand Center of Excellence in Physics, Ministry of Education, Bangkok 10400, Thailand

^cDepartamento de Fisica Teorica and Instituto de Fisica Teorica UAM/CSIC, Universidad Autonoma de Madrid, Cantoblanco, E-28049 Madrid, Spain

^dDepartment of Physics, Faculty of Science, Tokyo University of Science, 1-3, Kagurazaka, Shinjuku-ku, Tokyo 162-8601, Japan

E-mail: antoniod@nu.ac.th, nesseris@nbi.dk, shinji@rs.kagu.tus.ac.jp

Received March 30, 2012

Accepted April 28, 2012

Published May 24, 2012

Abstract. We place observational constraints on models with the late-time cosmic acceleration based on a number of parametrizations allowing fast transitions for the equation of state of dark energy. In addition to the model of Linder and Huterer where the dark energy equation of state w monotonically grows or decreases in time, we propose two new parametrizations in which w has an extremum. We carry out the likelihood analysis with the three parametrizations by using the observational data of supernovae type Ia, cosmic microwave background, and baryon acoustic oscillations. Although the transient cosmic acceleration models with fast transitions can give rise to the total chi square smaller than that in the Λ -Cold-Dark-Matter (Λ CDM) model, these models are not favored over Λ CDM when one uses the Akaike information criterion which penalizes the extra degrees of freedom present in the parametrizations.

Keywords: dark energy theory, supernova type Ia - standard candles

Contents

1	Introduction	1
2	Parametrizations of dark energy	2
3	Data analysis	5
4	Observational constraints on Model 1	6
5	Observational constraints on Model 2	9
6	Observational constraints on Model 3	11
7	Conclusions	14

1 Introduction

The discovery of the late-time cosmic acceleration [1] opened up a new research arena for cosmologists, astrophysicists, and particle physicists. From the viewpoint of particle physics the cosmological constant naturally appears as a vacuum energy of quantum fields, but its energy scale is usually very different from the observed dark energy scale [2]. As an alternative to the cosmological constant, dynamical dark energy models — such as quintessence [3], k-essence [4], $f(R)$ gravity [5], $f(R, \mathcal{G})$ gravity [6], DGP braneworld [7], and Galileon [8] — have been proposed. These models give rise to a time-varying equation of state $w(a)$ of dark energy, where a is the scale factor in the Friedmann-Lemaître-Robertson-Walker (FLRW) cosmological background [9].

At the background level it is possible to discriminate between a host of dark energy models by confronting $w(a)$ with the observations of Supernova type Ia (SN Ia), Cosmic Microwave Background (CMB), and Baryon Acoustic Oscillations (BAO). For this purpose several different parametrizations of $w(a)$ have been proposed — which are mostly based on two parameters w_0 and w_1 [10–15] (see refs. [16, 17] for the parametrizations of the Hubble parameter H or the luminosity distance D_L instead of w). A well known example is the so-called Chevalier-Polarski-Linder (CPL) parametrization $w(a) = w_0 + w_1(1 - a)$ [11, 13], where w_0 is the value of w today ($a = 1$). The 2-parameter parametrizations have been widely used for constraining the property of dark energy [18–20].

With two parameters one usually fixes w_0 and the value of w in the asymptotic past ($= w_p$). In this case it is generally difficult to accommodate the time a_t and the width τ of the transition in two asymptotic regimes. Bassett et al. [21] first proposed a 4-parameter parametrization involving a_t and τ . Corasaniti and Copeland [22] further developed this issue and proposed a *kink* parametrization given by $w(a) = w_0 + (w_p - w_0)[(1 + e^{a_t/\tau})(1 - e^{(1-a)/\tau})][(1 + e^{(a_t-a)/\tau})(1 - e^{1/\tau})]^{-1}$. This allows for quintessence models with tracker solutions having a rapid transition [23, 24], which is difficult to be addressed by the 2-parameter parametrization.

Bassett et al. [25] carried out the likelihood analysis with the kink parametrization by using the Gold SN Ia data [26] in 2004. They found that the best-fit corresponds to the case in which w is nearly constant ($w \sim w_p = -0.41$) for the redshift z larger than 0.1 and

rapidly decreases toward $w_0 \sim -2.85$ for $z < 0.1$. This evolution of w is outside the limits of the two-parameter parametrizations, which implies that two parameters are not generally sufficient to implement such a rapid transition.¹ Corasaniti et al. [33] also showed that the rapidly varying equation of state is consistent with the CMB and large-scale structure data accumulated by 2004.

For the kink parametrization the Hubble parameter H cannot be derived analytically in terms of a function of a . Instead Linder and Huterer (LH) [34] proposed the 4-parameter parametrization $w(a) = w_f + (w_p - w_f)[1 + (a/a_t)^{1/\tau}]^{-1}$, which also allows a rapid transition (where w_f is the value of w in the asymptotic future). In this case there exists an explicit integrated form of $H(a)$ with respect to a , so it is technically convenient. Moreover this parametrization can accommodate tracker scaling solutions ($w_p = 0$) with the rapid decrease of w [22, 23] and thawing quintessence models ($w_p = -1$) with the fast growth of w [35, 36].

For both the kink and the LH parametrizations the dark energy equation of state either increases or decreases monotonically. Meanwhile there are some models in which w has a minimum — such as quintessence [23], $f(R)$ gravity [37], and coupled dark energy [38] models. In order to implement models in which w has an extremum, we propose two new parametrizations given in eqs. (2.7) and (2.12) below. These are based on four parameters a_t , τ , w_p , and w_0 , which allow fast transitions of w . Moreover, in both cases, there exists analytic expression of the Hubble parameter.²

In this paper we shall place constraints on the model parameters of the LH parametrization (2.5) as well as those of the parametrizations (2.7) and (2.12) by using the recent observational data of SN Ia, CMB, and BAO. In each model the five parameters a_t , τ , w_p , w_0 (or w_f), and $\Omega_m^{(0)}$ (today's density parameter of non-relativistic matter) are varied in the likelihood analysis. We also carry out the 4-parameter space analysis by fixing w_0 with a number of different values between -1 and 0 . In order to accommodate the thawing-type models with fast transitions, we shall further set $w_p = -1$ and study the viability of the models (2.7) and (2.12) (including transient acceleration models) in the 3-parameter space. Note that the observational constraints on kink-like parametrizations different from those mentioned above (like those based on the deceleration parameter q) have been studied by a number of authors [40–44].

This paper is organized as follows. In section 2 we present the three parametrizations of $w(a)$ as well as the corresponding Hubble parameter $H(a)$. In section 3 we show the method of our likelihood analysis to confront the models with observations. In sections 4, 5, 6 we place observational constraints on the model parameters of the parametrizations (2.5), (2.7), and (2.12), respectively. Section 7 is devoted to conclusions.

2 Parametrizations of dark energy

We consider the flat FLRW background described by the line element $ds^2 = -dt^2 + a^2(t)d\mathbf{x}^2$, where t is cosmic time. We take into account dark energy with the time-varying equation of state $w(a)$ and non-relativistic matter with the density parameter $\Omega_m^{(0)}$ today. We assume

¹In some of quintessence and k-essence models such as thawing and tracker models, it is possible to derive the analytic forms of $w(a)$ approximately [28]–[32]. Apart from the tracker models with the inverse power-law potential [32], the field equation of state usually contains more than 3 free parameters [29–31].

²When the Hubble parameter is analytically available, one can also determine the Om diagnostic introduced in ref. [39].

that the dark energy density ρ_{DE} satisfies the continuity equation

$$\dot{\rho}_{\text{DE}} + 3H(1+w)\rho_{\text{DE}} = 0, \quad (2.1)$$

where a dot represents a derivative with respect to t , and $H = \dot{a}/a$ is the Hubble parameter. This equation can be written in an integrated form

$$\rho_{\text{DE}}(a) = \rho_{\text{DE}}^{(0)} \exp \left[\int_a^1 \frac{3}{\tilde{a}} (1+w) d\tilde{a} \right], \quad (2.2)$$

where $\rho_{\text{DE}}^{(0)}$ is the dark energy density today ($a = 1$). The energy density of non-relativistic matter is given by $\rho_m(a) = \rho_m^{(0)} a^{-3}$, where $\rho_m^{(0)}$ is its today's value.

The Friedmann equation gives

$$3H^2 = 8\pi G(\rho_m + \rho_{\text{DE}}), \quad (2.3)$$

where G is the gravitational constant. This can be written as

$$\frac{H^2(a)}{H_0^2} = \Omega_m^{(0)} a^{-3} + (1 - \Omega_m^{(0)}) \exp \left[\int_a^1 \frac{3}{\tilde{a}} (1+w) d\tilde{a} \right], \quad (2.4)$$

where H_0 is the present value of H , $\Omega_m^{(0)} = 8\pi G\rho_m^{(0)}/(3H_0^2)$, and we used the fact that $8\pi G\rho_{\text{DE}}^{(0)}/(3H_0^2) = 1 - \Omega_m^{(0)}$.

Next, we study the parametrization of dark energy allowing fast evolution of w . One of the examples is given by [34]

$$w(a) = w_f + \frac{w_p - w_f}{1 + (a/a_t)^{1/\tau}} \quad (\text{Model 1}), \quad (2.5)$$

where $a_t (> 0)$ is the scale factor at the transition epoch, and $\tau (> 0)$ characterizes the width of the transition. In the asymptotic past ($a \rightarrow 0$) and future ($a \rightarrow \infty$) one has $w \rightarrow w_p$ and $w \rightarrow w_f$, respectively. For the parametrization (2.5) the r.h.s. of eq. (2.4) is integrated to give

$$\frac{H^2(a)}{H_0^2} = \Omega_m^{(0)} a^{-3} + (1 - \Omega_m^{(0)}) \times a^{-3(1+w_p)} \left(\frac{a^{1/\tau} + a_t^{1/\tau}}{1 + a_t^{1/\tau}} \right)^{3\tau(w_p - w_f)}, \quad (2.6)$$

which is convenient in confronting the model with observations.

However, the parametrization (2.5) does not accommodate the models in which w has an extremum. In order to address such cases, we propose the following parametrization

$$w(a) = w_p + (w_0 - w_p) \frac{a[1 - (a/a_t)^{1/\tau}]}{1 - a_t^{-1/\tau}} \quad (\text{Model 2}), \quad (2.7)$$

where $a_t > 0$, $\tau > 0$, and w_p, w_0 are the values of w in the asymptotic past and today, respectively. For the parametrization (2.7) the Hubble parameter can be expressed as

$$\frac{H^2(a)}{H_0^2} = \Omega_m^{(0)} a^{-3} + (1 - \Omega_m^{(0)}) a^{-3(1+w_p)} \exp[f(a)], \quad (2.8)$$

where

$$f(a) = 3(w_0 - w_p) \times \frac{1 + (1 - a_t^{-1/\tau})\tau + a\{[(a/a_t)^{1/\tau} - 1]\tau - 1\}}{(1 - a_t^{-1/\tau})(1 + \tau)}. \quad (2.9)$$

The equation of state (2.7) has an extremum at

$$a_* = \left(\frac{\tau}{\tau + 1}\right)^\tau a_t, \quad (2.10)$$

with the value

$$w(a_*) = w_p + \frac{(w_0 - w_p)\tau^\tau(\tau + 1)^{-\tau-1}a_t}{1 - a_t^{-1/\tau}}. \quad (2.11)$$

If $0 < a_t < 1$ and $w_p < w_0$, or, $a_t > 1$ and $w_p > w_0$, then w has a minimum at $a = a_*$. On the other hand, if $0 < a_t < 1$ and $w_p > w_0$, or, $a_t > 1$ and $w_p < w_0$, w has a maximum at $a = a_*$.

For the models characterized by $w_p > w_0$ with a minimum of w at $0 < a_* < 1$ (such as quintessence models in ref. [23]), the transition redshift needs to satisfy the condition $a_t > 1$. From eq. (2.10) it follows that $a_t/e < a_* < a_t$ and hence $a_* > 1/e$. This means that, for $w_p > w_0$, the parametrization (2.7) does not accommodate the case in which w has a minimum at low redshifts. In order to improve this shortcoming, we shall also consider the following parametrization

$$w(a) = w_p + (w_0 - w_p) \frac{a^{1/\tau}[1 - (a/a_t)^{1/\tau}]}{1 - a_t^{-1/\tau}} \quad (\text{Model 3}), \quad (2.12)$$

where $a_t > 0$ and $\tau > 0$. Then w has an extremum at

$$a_* = \frac{a_t}{2^\tau}, \quad (2.13)$$

with the value

$$w(a_*) = w_p + \frac{1}{4} \frac{(w_0 - w_p)a_t^{1/\tau}}{1 - a_t^{-1/\tau}}. \quad (2.14)$$

The equation of state has a minimum either for $0 < a_t < 1$ and $w_p < w_0$, or, for $a_t > 1$ and $w_p > w_0$. Since $a_* \rightarrow 0$ for $\tau \gg 1$, we can cover the case of small a_* even for $a_t > 1$ and $w_p > w_0$.

The Hubble parameter corresponding to the parametrization (2.12) is given by eq. (2.8), where the function $f(a)$ is

$$f(a) = 3(w_0 - w_p)\tau \times \frac{2 - a_t^{-1/\tau} + a^{1/\tau}[(a/a_t)^{1/\tau} - 2]}{2(1 - a_t^{-1/\tau})}. \quad (2.15)$$

In the regime $0 < a < 1$ the parametrizations (2.5), (2.7), and (2.12) can recover the CPL parametrization $w(a) = w_0 + w_1(1 - a)$ in the limit that $a_t \gg 1$ (with $\tau = 1$ for Model 1 and Model 3).

3 Data analysis

In this section we explain the method employed to constrain Models 1, 2, and 3 observationally. In our analysis we use the three datasets: 1) the SN Ia (Constitution [45]); 2) the CMB shift parameters (WMAP7) [19]; 3) the BAO (SDSS7) [46]. The flat Universe is assumed throughout the analysis.

In SN Ia observations the apparent magnitude $m(z)$ at peak brightness is related with the luminosity distance $d_L(z) = (1+z) \int_0^z H^{-1}(\tilde{z}) d\tilde{z}$ through $m(z) = M + 5 \log_{10}(d_L(z)/10 \text{ pc})$, where $z = 1/a - 1$ is the redshift and M is the absolute magnitude [1]. We define the distance modulus

$$\mu(z) \equiv m(z) - M = 5 \log_{10}[H_0 d_L(z)] + \mu_0, \quad (3.1)$$

where $\mu_0 = 42.38 - 5 \log_{10} h$ with $h = H_0/[100 \text{ km sec}^{-1} \text{ Mpc}^{-1}]$. The chi square associated with SN Ia observations is given by

$$\chi_{\text{SN Ia}}^2 = \sum_{i=1}^N \frac{\mu_{\text{obs}}(z_i) - \mu(z_i)}{\sigma_{\mu,i}^2}, \quad (3.2)$$

where N is the number of the SN Ia dataset, $\mu_{\text{obs}}(z_i)$ are the observed values of the distance modulus, and $\sigma_{\mu,i}$ are the errors on the data. We employ the Constitution dataset with the total of 397 SN Ia in order to find the minimum of (3.2) and the corresponding best-fit parameters.

The position of the CMB acoustic peaks can be quantified by the following two parameters [47]

$$\mathcal{R} = \sqrt{\Omega_m^{(0)}} \int_0^{z_*} \frac{dz}{H(z)/H_0}, \quad l_a = \frac{\pi d_a^{(c)}(z_*)}{r_s(z_*)}, \quad (3.3)$$

where z_* is the redshift at the decoupling epoch, $d_a^{(c)}(z_*) = \mathcal{R}/[H_0 \sqrt{\Omega_m^{(0)}}]$ is the comoving angular diameter distance to the last scattering surface, and $r_s(z_*)$ is the sound horizon defined by

$$r_s(z_*) = \int_{z_*}^{\infty} \frac{dz}{H(z) \sqrt{3\{1 + 3\Omega_b^{(0)}/[4\Omega_\gamma^{(0)}(1+z)]\}}}. \quad (3.4)$$

Here $\Omega_b^{(0)}$ and $\Omega_\gamma^{(0)}$ are the density parameters of baryons and photons, respectively. For the redshift z_* there exists the following fitting formula [48]

$$z_* = 1048 [1 + 0.00124(\Omega_b^{(0)} h^2)^{-0.738}] [1 + g_1 (\Omega_m^{(0)} h^2)^{g_2}], \quad (3.5)$$

where $g_1 = 0.0783 (\Omega_b^{(0)} h^2)^{-0.238}/[1 + 39.5 (\Omega_b^{(0)} h^2)^{0.763}]$ and $g_2 = 0.560/[1 + 21.1 (\Omega_b^{(0)} h^2)^{1.81}]$. The chi square for the WMAP7 measurement is

$$\chi_{\text{CMB}}^2 = \mathbf{X}_{\text{CMB}}^T \mathbf{C}_{\text{CMB}}^{-1} \mathbf{X}_{\text{CMB}}, \quad (3.6)$$

where $\mathbf{X}_{\text{CMB}}^T = (l_a - 302.09, \mathcal{R} - 1.725, z_* - 1091.3)$, and the inverse covariance matrix is given by [19]

$$\mathbf{C}_{\text{CMB}}^{-1} = \begin{pmatrix} 2.305 & 29.698 & -1.333 \\ 29.698 & 6825.27 & -113.18 \\ -1.333 & -113.18 & 3.414 \end{pmatrix}. \quad (3.7)$$

The BAO observations constrain the ratio $r_{\text{BAO}}(z) \equiv r_s(z_d)/D_V(z)$, where $r_s(z_d)$ is the sound horizon at which the baryons are released from the Compton drag of photons (denoted as the redshift z_d). $D_V(z)$ is the effective BAO distance defined by $D_V(z) \equiv [d_a^{(c)}(z)^2 z/H(z)]^{1/3}$ [49], where $d_a^{(c)}(z) = \int_0^z H^{-1}(\tilde{z})d\tilde{z}$. For the redshift z_d there is the following fitting formula [50]

$$z_d = \frac{1291 (\Omega_m^{(0)} h^2)^{0.251}}{1 + 0.659 (\Omega_m^{(0)} h^2)^{0.828}} [1 + b_1 (\Omega_b^{(0)} h^2)^{b_2}], \quad (3.8)$$

where $b_1 = 0.313 (\Omega_m^{(0)} h^2)^{-0.419} [1 + 0.607 (\Omega_m^{(0)} h^2)^{0.674}]$ and $b_2 = 0.238 (\Omega_m^{(0)} h^2)^{0.223}$. The chi square associated with the BAO measurement is given by

$$\chi_{\text{BAO1}}^2 = \mathbf{X}_{\text{BAO}}^T \mathbf{C}_{\text{BAO}}^{-1} \mathbf{X}_{\text{BAO}}, \quad (3.9)$$

where $\mathbf{X}_{\text{BAO}}^T = (r_{\text{BAO}}(0.2) - 0.1905, r_{\text{BAO}}(0.35) - 0.1097)$, and the inverse covariance matrix is [46]

$$\mathbf{C}_{\text{BAO}}^{-1} = \begin{pmatrix} 30124 & -17227 \\ -17227 & 86977 \end{pmatrix}. \quad (3.10)$$

We also use the BAO data from the WiggleZ and 6dFGS surveys. These data are given in terms of $A(z)$, where its theoretical value is

$$A_{\text{th}}(z) \equiv \frac{D_V(z) \sqrt{\Omega_m^{(0)} H_0^2}}{z}, \quad (3.11)$$

and the data are $A_{\text{WiggleZ}}(z = 0.6) = 0.452 \pm 0.018$ [51] and $A_{\text{6dFGS}}(z = 0.106) = 0.526 \pm 0.028$ [52]. The chi-square is given by

$$\chi_{\text{BAO2}}^2 = \sum_{i=1}^2 \left(\frac{A(z_i) - A_{\text{th}}(z_i)}{\sigma_i} \right)^2. \quad (3.12)$$

Therefore, the total chi-square from the three datasets is

$$\chi^2 = \chi_{\text{SNIa}}^2 + \chi_{\text{CMB}}^2 + \chi_{\text{BAO1}}^2 + \chi_{\text{BAO2}}^2. \quad (3.13)$$

The best-fit corresponds to the model parameters for which the χ^2 is minimized.

4 Observational constraints on Model 1

We place observational constraints on Model 1 according to the method explained in section 3.

We first vary the 5 parameters w_p, w_f, a_t, τ , and $\Omega_m^{(0)}$ in the likelihood analysis. The priors on each parameter are set to be $-10 \leq w_p \leq 10$, $-10 \leq w_f \leq 10$, $a_t > 0$, $\tau > 0$, and $0.15 < \Omega_m^{(0)} < 0.4$. We find that the best-fit parameters are

$$\begin{aligned} w_p &= 0.141866, & w_f &= -1.02862, & a_t &= 0.132023, \\ \tau &= 0.360069, & \Omega_m^{(0)} &= 0.290346, \end{aligned} \quad (4.1)$$

with $\chi^2 = 467.77$. In figure 1 we plot the evolution of w for the best-fit case [line (a)]. Initially there is a period where w stays nearly constant ($w \simeq 0.14$), which is followed by

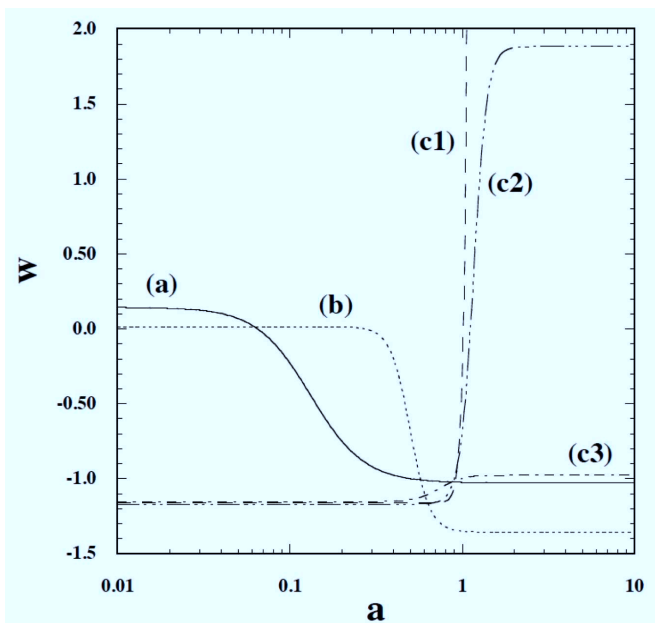


Figure 1. The dark energy equation of state w versus the scale factor a for Model 1 with several different model parameters. The line (a) corresponds to the best-fit case of eq. (4.1) derived by varying the 5 parameters $w_p, w_f, a_t, \tau, \Omega_m^{(0)}$ in the likelihood analysis. The line (b) shows the best-fit derived with the priors $w_p \geq 0$ and $a_t \geq 0.5$. The lines (c1), (c2), (c3) represent the best-fits where the 4 parameters $w_p, a_t, \tau, \Omega_m^{(0)}$ are varied with the present value of the equation of state fixed at $w_0 = -1/3, -0.7, -1$, respectively.

the decrease of w around the redshift z larger than 10. The dark energy equation of state crosses the cosmological constant boundary ($w = -1$) around $z = 1$ and it approaches the asymptotic value $w_f = -1.028$.

If w starts to evolve from the value larger than 0 in the deep matter era, it is required that the transition to the regime $w \approx -1$ occurs in the early cosmological epoch (for z larger than 1). In fact, if we carry out the likelihood analysis with the priors $w_p \geq 0$ and $a_t \geq 0.5$, the best-fit model parameters are found to be

$$\begin{aligned} w_p &= 0.0120045, & w_f &= -1.35856, & a_t &= 0.5, \\ \tau &= 0.130893, & \Omega_m^{(0)} &= 0.300473, & & \end{aligned} \quad (4.2)$$

with $\chi^2 = 505.983$. In this case, the bound on a_t is saturated at $a_t = 0.5$ and the best-fit χ^2 is much larger than that corresponding to eq. (4.1). Since $\tau \ll 1$, the transition from the regime $w \geq 0$ to the regime $w \approx -1$ occurs quite rapidly. In figure 1 we compare the behavior of the two best-fits in eqs. (4.1) and (4.2).

The likelihood analysis of Bassett et al. [25] for the kink parametrization, with the SN Ia and CMB data accumulated by 2004, showed that the best fit corresponds to the fast transition in low redshifts ($z < 0.1$). However, inclusion of the BAO data as well as the more updated SN Ia and CMB data, seems to point towards a much earlier transition from the regime $w \sim 0$ to the regime close to $w = -1$.

In order to study the possibility of the late-time transition further, we also study the case in which the value of w today ($= w_0$) is fixed. Since $w_f = a_t^{1/\tau} [w_0(1 + a_t^{-1/\tau}) - w_p]$, the

w_0	w_p	a_t	τ	$\Omega_m^{(0)}$	χ^2
0	-1.04279	1.20514	0.00277414	0.276338	470.825
-1/3	-1.16253	1.31208	0.0502325	0.280804	471.530
-0.5	-1.17027	1.30959	0.0659688	0.281219	470.996
-0.6	-1.17165	1.26349	0.0779737	0.281295	470.707
-0.7	-1.17077	1.16698	0.0907055	0.281248	470.456
-0.8	-1.16655	1.18425	0.116396	0.280961	470.276
-1	-1.15384	0.742678	0.15533	0.279799	470.387

Table 1. The best-fit model parameters (4 parameters in total) and χ^2 for Model 1 with several given values of w_0 .

parametrization (2.5) can be expressed as

$$w(a) = \frac{w_p + a^{1/\tau}[w_0(1 + a_t^{-1/\tau}) - w_p]}{1 + (a/a_t)^{1/\tau}}. \quad (4.3)$$

For several given values of w_0 we vary the 4 parameters w_p , a_t , τ , and $\Omega_m^{(0)}$ with the priors $-10 \leq w_p \leq 10$, $a_t > 0$, $\tau > 0$, and $0.15 < \Omega_m^{(0)} < 0.4$. In table 1 the best-fit model parameters and the corresponding χ^2 are shown for $w_0 = 0, -1/3, -0.5, -0.6, -0.7, -0.8, -1$. In figure 1 we also plot w versus a for several different best-fit cases ($w_0 = -1/3, -0.7, -1$).

For the values of w_0 between -1 and 0 , the initial evolution of w for each case shown in table 1 exhibits a common property. The dark energy equation of state is nearly constant with w less than -1 during the deep matter era, which is followed by the growth of w in the low-redshift regime ($z \lesssim 1$). The parameter τ tends to be smaller for larger w_0 , so that the transition becomes sharper. This property can be confirmed by comparing the three best-fit cases (c1)-(c3) in figure 1.

In table 1 we find that χ^2 is more or less similar for different choices of w_0 between -1 and 0 . The best-fit Λ CDM model corresponds to $\Omega_m^{(0)} = 0.269431$ with $\chi^2 = 471.89$, whose χ^2 is larger than those given in table 1. This implies that the transient cosmic acceleration models with rapid transitions of w are not excluded by the current observational data.

We need to caution, however, that the parametrization (4.3) with given w_0 has 4 free parameters to fit the models with the data, while the Λ CDM model has only one free parameter ($\Omega_m^{(0)}$). In order to compare the models with different number of free parameters, we employ the Akaike Information Criterion (AIC) [53]. The AIC is defined as

$$\text{AIC} = \chi_{\min}^2 + 2\mathcal{P}, \quad (4.4)$$

where χ_{\min}^2 is the minimum value of χ^2 , and \mathcal{P} is the number of free parameters for each model. For smaller AIC the model is more favored. If the difference of AIC between two models is in the range $0 < \Delta(\text{AIC}) < 2$, the models are considered to be equivalent. On the other hand, if $\Delta(\text{AIC}) > 2$, one model is favored over another one.

The flat Λ CDM model corresponds to $\text{AIC} = 473.89$, whereas the transient acceleration models in table 1 give rise to larger values of AIC (e.g., $\text{AIC} = 478.825$ for $w_0 = 0$). The best-fit case (4.1) with 5 parameters corresponds to $\text{AIC} = 477.77$. According to the AIC, Model 1 with 5 or 4 free parameters is not favored over the Λ CDM model.

w_0	w_p	a_t	τ	$\Omega_m^{(0)}$	χ^2
0	-0.96206	0.93842	0.04200	0.27847	473.130
-1/3	-1.05556	0.90118	0.06302	0.28045	471.638
-0.5	-1.14904	0.80038	0.07330	0.28111	471.001
-0.7	-1.04574	0.87618	0.14101	0.28095	470.468
-0.9	-0.97634	0.92387	0.77675	0.28064	470.246

Table 2. The best-fit model parameters (4 parameters in total) and χ^2 for Model 2 with several given values of w_0 .

5 Observational constraints on Model 2

Let us proceed to observational constraints on Model 2. We first vary the 5 parameters w_p, w_0, a_t, τ , and $\Omega_m^{(0)}$ in the likelihood analysis. We set the priors on each parameter, as $-10 \leq w_p \leq 10$, $-10 \leq w_0 \leq 10$, $a_t > 0$, $\tau > 0$, and $0.15 < \Omega_m^{(0)} < 0.4$. The best-fit parameters are found to be

$$\begin{aligned} w_p &= -1.10237, & w_0 &= -0.906508, & a_t &= 0.739325, \\ \tau &= 0.505998, & \Omega_m^{(0)} &= 0.280583, \end{aligned} \quad (5.1)$$

with $\chi^2 = 470.241$. In this case χ^2 is smaller than that in the Λ CDM model, but it is larger than that in the best-fit case (4.1) of Model 1.

In figure 2 the evolution of w for the parameters (5.1) is plotted as the solid line (a). As we showed in section 2, w has a minimum at a_* given in eq. (2.10) either for (i) $0 < a_t < 1$, $w_p < w_0$, or (ii) $a_t > 1$, $w_p > w_0$. The best-fit model parameters (5.1) correspond to the case (i) with $a_* = 0.43$. The equation of state starts from a phantom value $w_p = -1.10237$, which is followed by mild decrease of w . For $a > a_*$ it starts to increase and reaches the present value $w_0 = -0.906508$.

The above behavior of w is different from that for the best-fit Model 1 with 5 parameters varied. As we see in figure 1 the best-fit parameters in Model 1 satisfy the condition $w_p > w_0$, but in this case Model 2 gives rise to a minimum only for $a_t > 1$. Since a_* is limited in the range $a_t/e < a_* < a_t$ and also τ is required to be large ($\tau \gg 1$) to have small a_* , it becomes more difficult to fit w with the observational data for $a_t > 1$ and $w_p > w_0$. If $w_p > w_0$ and $0 < a_t < 1$, w has a maximum at $a = a_*$. However, such cases are also difficult to be compatible with the observational data.

By choosing several different values of w_0 ($= 0, -1/3, -0.5, -0.7, -0.9$), we also vary the 4 parameters $w_p, a_t, \tau, \Omega_m^{(0)}$ in the likelihood analysis. The priors are set to be $-10 \leq w_p \leq 10$, $a_t > 0$, $\tau > 0$, and $0.15 < \Omega_m^{(0)} < 0.4$. In table. 2 we show the best-fit parameters and χ^2 for each w_0 . In all cases we find that $0 < a_t < 1$ and $w_p < w_0$, so that w has a minimum at $0 < a_* < 1$.

In figure 2 we show the variation of w for the best-fit cases with $w_0 = 0$ and $w_0 = -0.7$ as the lines (b1) and (b2), respectively. The growth of w in the regime $a > a_*$ is sharper for larger values of w_0 . This reflects the fact that, in table 2, τ gets smaller for w_0 increased. We also note that the models with larger w_0 tend to be disfavored because of the increase of χ^2 seen in table 2.

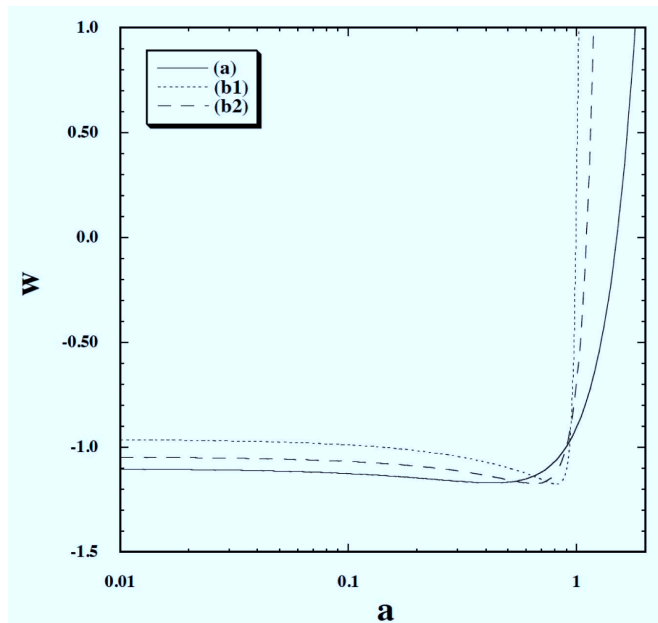


Figure 2. The dark energy equation of state w versus a for Model 2. The line (a) corresponds to the 5-parameter best-fit case given in eq. (5.1). The lines (b1) and (b2) show the best-fits where the 4 parameters $w_p, a_t, \tau, \Omega_m^{(0)}$ are varied with $w_0 = 0, -0.7$, respectively.

w_0	w_p	a_t	τ	$\Omega_m^{(0)}$	χ^2
0	-1	0.940663	0.0319267	0.277496	472.984
-1/3	-1	0.916762	0.0689972	0.280277	471.702
-0.5	-1	0.909223	0.0938171	0.280760	471.074
-0.7	-1	0.901454	0.1517700	0.280844	470.476
-0.9	-1	0.897160	0.7207540	0.280662	470.245

Table 3. The best-fit model parameters (3 parameters in total) and χ^2 for Model 2 with $w_p = -1$ and several given values of w_0 .

In addition to w_0 , we also fix w_p to be -1 and vary the 3 parameters $a_t, \tau, \Omega_m^{(0)}$. In table 3 we present the best-fit model parameters for several different choices of w_0 (> -1). In all cases the transition scale factor is in the range $0 < a_t < 1$, so that w has a minimum for $0 < a_* < 1$. In fact, the evolution of w starting from -1 and having a minimum by today is present for dark energy models based on $f(R)$ theories [37] (although w does not continuously grow for $a > 1$). Table 3 shows that, for larger w_0 , τ tends to be smaller, whereas χ^2 gets larger.

In figure 3 we illustrate the 1σ and 2σ observational contours in the (a_t, τ) plane for $w_p = -1$, $w_0 = -1/3$, and $\Omega_m^{(0)} = 0.280277$. This is the marginal case in which the Universe enters the phase of cosmic deceleration today. The redshift and the width of the transition are constrained to be $0.87 < a_t < 0.99$ and $0 < \tau < 0.18$ (68% CL). Unless the rapid transition occurs at the redshift close to today, the model is not compatible with the observational data. For larger τ the values of w at $a = a_*$ start to deviate from -1 , so that those cases are more difficult to satisfy observational constraints.

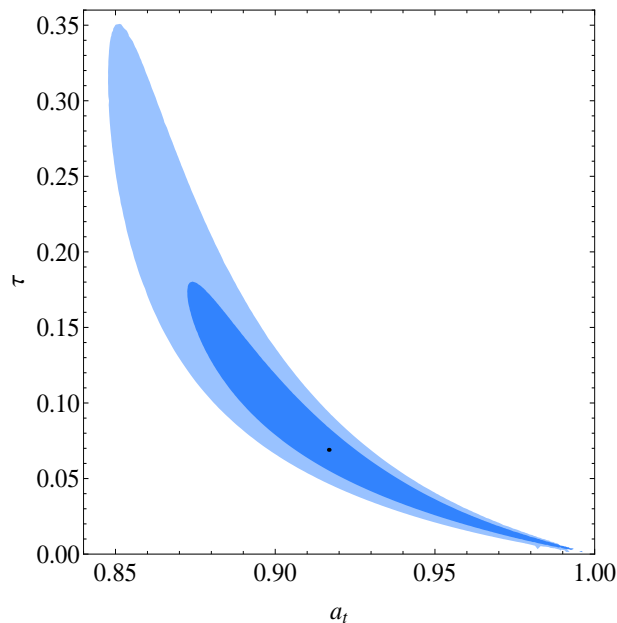


Figure 3. The 1σ (inside) and 2σ (outside) likelihood contours in the (a_t, τ) plane derived by varying the 2 parameters a_t and τ with $w_p = -1$, $w_0 = -1/3$, and $\Omega_m^{(0)} = 0.280277$ for Model 2. The black point corresponds to the best-fit case.

As mentioned in section 4, the AIC for the flat Λ CDM model is $\text{AIC} = 473.89$. For the 5-parameter best-fit case in eq. (5.1) and for the 4-parameter and 3-parameter best-fit cases given in tables 2 and 3, the AIC in each model is larger than that in the Λ CDM model with the difference more than 2. Hence the AIC criterion shows that the Λ CDM is generally favored over Model 2.

6 Observational constraints on Model 3

Finally we proceed to observational constraints on Model 3. When the 5 parameters $w_p, w_0, a_t, \tau, \Omega_m^{(0)}$ are varied in the likelihood analysis, we set the same priors as those given in Model 2. The best-fit parameters are found to be

$$\begin{aligned} w_p &= -1.10733, & w_0 &= -0.897454, & a_t &= 0.737871, \\ \tau &= 0.652107, & \Omega_m^{(0)} &= 0.28053, & & \end{aligned} \quad (6.1)$$

with $\chi^2 = 470.235$.

As we see in figure 4, the evolution of w corresponding to eq. (6.1) is similar to that for the best-fit parameters (5.1) of Model 2. Since $0 < a_t < 1$ and $w_p < w_0$ for the model parameters (6.1), w has a minimum at $a_* = 0.47$. The difference between Models 2 and 3 is that even for $a_t > 1$ and $w_p > w_0$ the equation of state for Model 3 can take minima with smaller values of a_* given in eq. (2.13). However we find that the models with $a_t > 1$ and $\tau \gg 1$ are disfavored because $w(a_*)$ deviates from -1 .

For the 4-parameter parametrization with a number of different values of w_0 ($= 0, -1/3, -0.5, -0.7, -0.9$) we also vary the parameters $w_p, a_t, \tau, \Omega_m^{(0)}$ with the same priors used for Model 2. In table 4 we summarize the best-fit parameters as well as the χ^2 for each

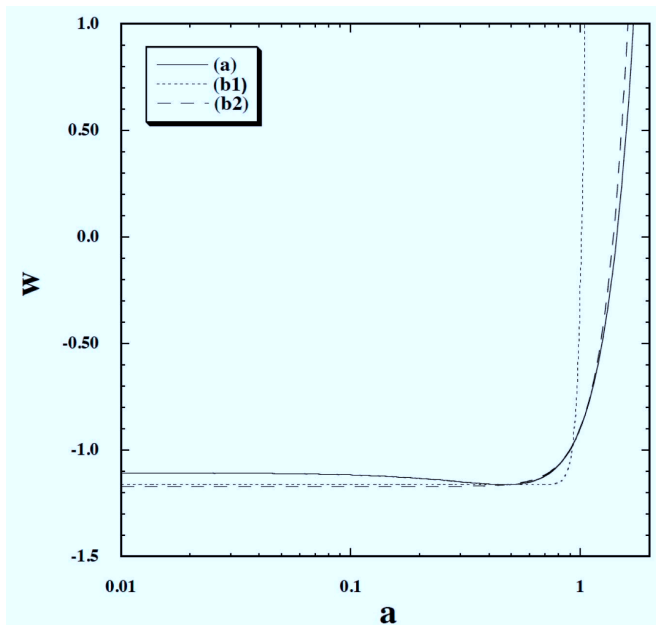


Figure 4. The dark energy equation of state w versus a for Model 3. The line (a) represents the 5-parameter best-fit case given in eq. (6.1), whereas the lines (b1) and (b2) correspond to the best-fits derived by varying the 4 parameters $w_p, a_t, \tau, \Omega_m^{(0)}$ with $w_0 = -1/3, -0.9$, respectively.

w_0	w_p	a_t	τ	$\Omega_m^{(0)}$	χ^2
0	-1.04278	3.86853	5.86338×10^{-13}	0.27634	470.825
-1/3	-1.16195	0.68613	0.10267	0.28079	471.533
-0.5	-1.16009	0.78777	0.15968	0.28113	471.001
-0.7	-1.06189	0.86545	0.35609	0.28086	470.468
-0.9	-1.17212	2.75038	0.22092	0.28049	470.234

Table 4. The best-fit model parameters (4 parameters in total) and χ^2 for Model 3 with several given values of w_0 .

w_0 . For $w_0 = -1/3, -0.5, -0.7$ one has $0 < a_t < 1$ and $w_p < w_0$, in which cases w has minima at $0 < a_* < 1$. If $w_0 > -0.5$, the growth of w in the regime $a > a_*$ is very rapid (see the line (b1) in figure 4).

For the best-fit parameters corresponding to $w_0 = 0, -0.9$ one has $a_t > 1$ and $w_p < w_0$. In those cases w has maxima at a_* larger than 1 and hence w is a growing function for $a < 1$. Since τ is extremely small for $w_0 = 0$, the transition of w occurs almost like a step function. However such an instant transition cannot be regarded as a realistic model of dark energy. For $w_0 = -0.9$, w has a maximum ($w(a_*) = 5.5$) at $a_* = 2.4$. In this case the evolution of w is not very different from that for the best-fit case (6.1), apart from the fact that for $w_0 = -0.9$ the equation of state is a growing function in the regime $a < 1$.

We also vary the 3 parameters $a_t, \tau, \Omega_m^{(0)}$ by fixing w_p to be -1 for several different choices of $w_0 (> -1)$. In table 5 we show the best-fit values as well as χ^2 for each w_0 . In

w_0	w_p	a_t	τ	$\Omega_m^{(0)}$	χ^2
0	-1	0.918824	0.185756	0.277967	474.087
-1/3	-1	0.909047	0.249165	0.279820	472.013
-0.5	-1	0.904406	0.296622	0.280332	471.194
-0.7	-1	0.899265	0.398049	0.280590	470.495
-0.9	-1	0.901692	0.788501	0.280323	470.242

Table 5. The best-fit model parameters (3 parameters in total) and χ^2 for Model 3 with $w_p = -1$ and several given values of w_0 .

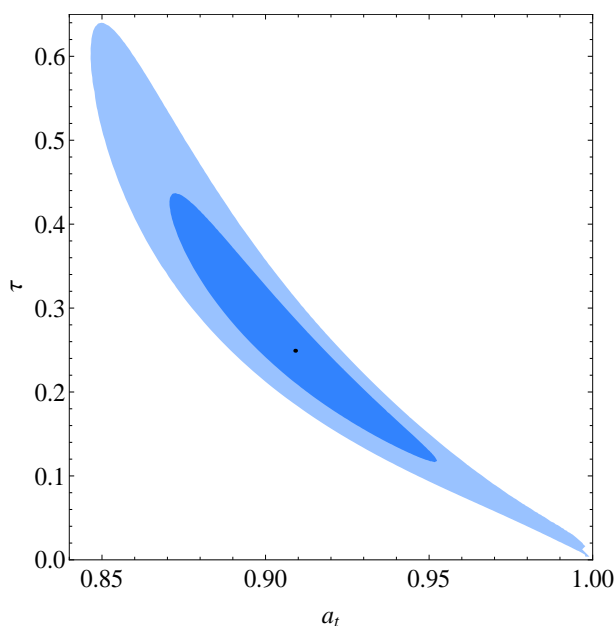


Figure 5. The 1σ (inside) and 2σ (outside) likelihood contours in the (a_t, τ) plane derived by varying the 2 parameters a_t and τ with $w_p = -1$, $w_0 = -1/3$, and $\Omega_m^{(0)} = 0.279820$ for Model 3. The black point corresponds to the best-fit case.

most cases the transition redshifts are around $a_t = 0.9$. As we increase w_0 the parameter τ gets smaller, so that the transition occurs more rapidly. For larger w_0 , χ^2 tends to be larger.

In figure 5 we plot observational bounds in the (a_t, τ) plane for $w_p = -1$, $w_0 = -1/3$, and $\Omega_m^{(0)} = 0.279820$. Comparing it to figure 3, we find that the larger values of τ can be allowed in Model 3. This reflects the fact that in Model 3 the values of $w(a_*)$ do not deviate from -1 significantly for $\tau \lesssim 0.5$. The two parameters are constrained to be $0.87 < a_t < 0.95$ and $0.12 < \tau < 0.44$ (68% CL).

For all the best-fit cases discussed above, the AIC is larger than that in the flat Λ CDM model. Hence Model 3 is not favored over the Λ CDM model according to the AIC.

7 Conclusions

In this paper we placed observational constraints on the three models allowing fast transitions of w , by using the data of SN Ia, CMB shift parameters, and BAO. Unlike the 2-parameter parametrization such as $w(a) = w_0 + w_1(1 - a)$, the parametrizations (2.5), (2.7), and (2.12) have two more parameters a_t and τ by which the time and the width of the transition can be accommodated. In Model 1 the dark energy equation of state monotonically increases or decreases in time, whereas in Models 2 and 3 w has either a minimum or a maximum depending on the values of w_p , w_0 , and a_t . For all these models the Hubble parameter H is analytically known in terms of functions of a .

When the 5 parameters $w_p, w_f, a_t, \tau, \Omega_m^{(0)}$ are varied in Model 1, the best-fit parameters are given by eq. (4.1) with $\chi^2 = 467.77$. This corresponds to the solid curve (a) in figure 1, in which case the equation of state enters the regime $w \sim -1$ in the early cosmological epoch. If we put the prior on the transition redshift as $a_t > 0.5$, χ^2 becomes significantly larger than that without a prior on a_t . This means that the late-time transition ($a_t > 0.5$) from the regime $w \sim 0$ to the regime $w \sim -1$ is disfavored observationally. If we vary the 4 parameters $w_p, a_t, \tau, \Omega_m^{(0)}$ with several different values of w_0 between -1 and 0 , the parameter τ tends to be smaller for increasing w_0 . Although the χ^2 in Model 1 with 5 or 4 parameters can be smaller than that in the Λ CDM model, the AIC shows that Model 1 is not favored over the Λ CDM model.

The best-fit parameters for Model 2 corresponds to the case in which w starts from a phantom value $w_p = -1.10$, takes a minimum -1.17 at $a_* = 0.43$, and grows to the value $w_0 = -0.91$ by today. This is different from the evolution of w for the best-fit parameters of Model 1. This difference mainly comes from the fact that, in the cases $w_p > w_0$ for Model 2, w has a minimum at a_* given by eq. (2.10) only for $a_t > 1$. While Model 2 can accommodate the late-time transition having a minimum of w , it is difficult to address the early sharp transition with $w_p > w_0$. The 4-parameter likelihood analysis for a number of fixed w_0 (between -1 and 0) leads to similar best-fit evolution of w to that for the 5-parameter best-fit case, with a faster transition for larger w_0 .

In Model 3 the equation of state has an extremum at $a_* = a_t/2^\tau$, which can be smaller than that for Model 2. If $w_p > w_0$, however, the early transition of w with a minimum requires the condition $\tau \gg 1$. This value of τ is too large to accommodate the early transition compatible with observations, because the minimum value of w tends to deviate from -1 . The 5-parameter likelihood analysis shows that the best-fit case in Model 3 is similar to that in Model 2. The likelihood results for 4 parameters (w_0 fixed) and for 3 parameters (w_0 and w_p fixed) also give rise to the similar results to those found in Model 2.

In Models 2 and 3 the AIC is always larger than that in the Λ CDM model with the difference more than 2. Hence the models with the late-time fast transition to the non-accelerating Universe are disfavored compared to the Λ CDM model. The joint data analysis based on SN Ia, CMB, and BAO prefers the models in which w do not deviate significantly from -1 in the low-redshift regime.

Although the minimum value of χ^2 in Model 1 with 5 parameters is smaller than those in Models 2 and 3, the minima in Models 2 and 3 are still inside the 1σ region corresponding to Model 1. Therefore we cannot prefer/exclude any parametrization with respect to any other one.

Recently it was shown that, in the framework of the CPL parametrization, the observational constraints on dark energy are sensitive to the presence of the cosmic curvature $\Omega_K^{(0)}$ [54]. They found that the CPL parametrization is not sufficiently flexible to model the

rapidly varying equation of state in low redshifts even for $\Omega_K^{(0)} \neq 0$ (see also ref. [43]). It will be of interest to study how the effect of the cosmic curvature affects the observational constraints on the models discussed in this paper. We leave this for future work.

Acknowledgments

We thank Takeshi Chiba for useful discussions. S. N. acknowledges support from the Madrid Regional Government (CAM) under the program HEPHACOS S2009/ESP-1473-02. S. T. is supported by the Grant-in-Aid for Scientific Research Fund of the Fund of the JSPS No 30318802 and Scientific Research on Innovative Areas (No. 21111006). S. T. thanks Reza Tavakol for warm hospitality during his stay in University of Queen Mary.

References

- [1] SUPERNOVA SEARCH TEAM collaboration, A.G. Riess et al., *Observational evidence from supernovae for an accelerating universe and a cosmological constant*, *Astron. J.* **116** (1998) 1009 [[astro-ph/9805201](#)] [[INSPIRE](#)];
SUPERNOVA COSMOLOGY PROJECT collaboration, S. Perlmutter et al., *Measurements of Ω and Λ from 42 high redshift supernovae*, *Astrophys. J.* **517** (1999) 565 [[astro-ph/9812133](#)] [[INSPIRE](#)].
- [2] S. Weinberg, *The cosmological constant problem*, *Rev. Mod. Phys.* **61** (1989) 1 [[INSPIRE](#)].
- [3] Y. Fujii, *Origin of the gravitational constant and particle masses in scale invariant scalar-tensor theory*, *Phys. Rev. D* **26** (1982) 2580 [[INSPIRE](#)];
C. Wetterich, *Cosmology and the fate of dilatation symmetry*, *Nucl. Phys. B* **302** (1988) 668 [[INSPIRE](#)];
B. Ratra and P. Peebles, *Cosmological consequences of a rolling homogeneous scalar field*, *Phys. Rev. D* **37** (1988) 3406 [[INSPIRE](#)];
T. Chiba, N. Sugiyama and T. Nakamura, *Cosmology with x -matter*, *Mon. Not. Roy. Astron. Soc.* **289** (1997) L5 [[astro-ph/9704199](#)] [[INSPIRE](#)];
P.G. Ferreira and M. Joyce, *Structure formation with a selftuning scalar field*, *Phys. Rev. Lett.* **79** (1997) 4740 [[astro-ph/9707286](#)] [[INSPIRE](#)];
R. Caldwell, R. Dave and P.J. Steinhardt, *Cosmological imprint of an energy component with general equation of state*, *Phys. Rev. Lett.* **80** (1998) 1582 [[astro-ph/9708069](#)] [[INSPIRE](#)].
- [4] C. Armendariz-Picon, T. Damour and V.F. Mukhanov, *k -inflation*, *Phys. Lett. B* **458** (1999) 209 [[hep-th/9904075](#)] [[INSPIRE](#)];
T. Chiba, T. Okabe and M. Yamaguchi, *Kinetically driven quintessence*, *Phys. Rev. D* **62** (2000) 023511 [[astro-ph/9912463](#)] [[INSPIRE](#)];
C. Armendariz-Picon, V.F. Mukhanov and P.J. Steinhardt, *A dynamical solution to the problem of a small cosmological constant and late time cosmic acceleration*, *Phys. Rev. Lett.* **85** (2000) 4438 [[astro-ph/0004134](#)] [[INSPIRE](#)].
- [5] S. Capozziello, *Curvature quintessence*, *Int. J. Mod. Phys. D* **11** (2002) 483 [[gr-qc/0201033](#)] [[INSPIRE](#)];
S. Capozziello, S. Carloni and A. Troisi, *Quintessence without scalar fields*, *Recent Res. Dev. Astron. Astrophys.* **1** (2003) 625 [[astro-ph/0303041](#)] [[INSPIRE](#)];
S.M. Carroll, V. Duvvuri, M. Trodden and M.S. Turner, *Is cosmic speed-up due to new gravitational physics?*, *Phys. Rev. D* **70** (2004) 043528 [[astro-ph/0306438](#)] [[INSPIRE](#)].
- [6] S.M. Carroll et al., *The cosmology of generalized modified gravity models*, *Phys. Rev. D* **71** (2005) 063513 [[astro-ph/0410031](#)] [[INSPIRE](#)];
S. Nojiri and S.D. Odintsov, *Modified Gauss-Bonnet theory as gravitational alternative for dark energy*, *Phys. Lett. B* **631** (2005) 1 [[hep-th/0508049](#)] [[INSPIRE](#)];

- A. De Felice and S. Tsujikawa, *Construction of cosmologically viable $f(G)$ dark energy models*, *Phys. Lett. B* **675** (2009) 1 [[arXiv:0810.5712](#)] [[INSPIRE](#)];
- A. De Felice and T. Suyama, *Vacuum structure for scalar cosmological perturbations in modified gravity models*, *JCAP* **06** (2009) 034 [[arXiv:0904.2092](#)] [[INSPIRE](#)];
- A. De Felice and T. Tanaka, *Inevitable ghost and the degrees of freedom in $f(R, G)$ gravity*, *Prog. Theor. Phys.* **124** (2010) 503 [[arXiv:1006.4399](#)] [[INSPIRE](#)].
- [7] G. Dvali, G. Gabadadze and M. Porrati, *4D gravity on a brane in 5D Minkowski space*, *Phys. Lett. B* **485** (2000) 208 [[hep-th/0005016](#)] [[INSPIRE](#)].
- [8] A. Nicolis, R. Rattazzi and E. Trincherini, *The Galileon as a local modification of gravity*, *Phys. Rev. D* **79** (2009) 064036 [[arXiv:0811.2197](#)] [[INSPIRE](#)];
C. Deffayet, G. Esposito-Farese and A. Vikman, *Covariant Galileon*, *Phys. Rev. D* **79** (2009) 084003 [[arXiv:0901.1314](#)] [[INSPIRE](#)];
A. De Felice and S. Tsujikawa, *Cosmology of a covariant Galileon field*, *Phys. Rev. Lett.* **105** (2010) 111301 [[arXiv:1007.2700](#)] [[INSPIRE](#)]; *Generalized Galileon cosmology*, *Phys. Rev. D* **84** (2011) 124029 [[arXiv:1008.4236](#)] [[INSPIRE](#)].
- [9] V. Sahni and A.A. Starobinsky, *The case for a positive cosmological Λ -term*, *Int. J. Mod. Phys. D* **9** (2000) 373 [[astro-ph/9904398](#)] [[INSPIRE](#)];
S.M. Carroll, *The cosmological constant*, *Living Rev. Rel.* **4** (2001) 1 [[astro-ph/0004075](#)];
T. Padmanabhan, *Cosmological constant: the weight of the vacuum*, *Phys. Rept.* **380** (2003) 235 [[hep-th/0212290](#)] [[INSPIRE](#)];
P. Peebles and B. Ratra, *The cosmological constant and dark energy*, *Rev. Mod. Phys.* **75** (2003) 559 [[astro-ph/0207347](#)] [[INSPIRE](#)];
E.J. Copeland, M. Sami and S. Tsujikawa, *Dynamics of dark energy*, *Int. J. Mod. Phys. D* **15** (2006) 1753 [[hep-th/0603057](#)] [[INSPIRE](#)];
T.P. Sotiriou and V. Faraoni, *$f(R)$ theories of gravity*, *Rev. Mod. Phys.* **82** (2010) 451 [[arXiv:0805.1726](#)] [[INSPIRE](#)];
A. De Felice and S. Tsujikawa, *$f(R)$ theories*, *Living Rev. Rel.* **13** (2010) 3 [[arXiv:1002.4928](#)] [[INSPIRE](#)];
S. Tsujikawa, *Modified gravity models of dark energy*, *Lect. Notes Phys.* **800** (2010) 99 [[arXiv:1101.0191](#)] [[INSPIRE](#)]; *Dark energy: investigation and modeling*, [arXiv:1004.1493](#) [[INSPIRE](#)].
- [10] D. Huterer and M.S. Turner, *Probing the dark energy: methods and strategies*, *Phys. Rev. D* **64** (2001) 123527 [[astro-ph/0012510](#)] [[INSPIRE](#)].
- [11] M. Chevallier and D. Polarski, *Accelerating universes with scaling dark matter*, *Int. J. Mod. Phys. D* **10** (2001) 213 [[gr-qc/0009008](#)] [[INSPIRE](#)].
- [12] J. Weller and A. Albrecht, *Future supernovae observations as a probe of dark energy*, *Phys. Rev. D* **65** (2002) 103512 [[astro-ph/0106079](#)] [[INSPIRE](#)].
- [13] E.V. Linder, *Exploring the expansion history of the universe*, *Phys. Rev. Lett.* **90** (2003) 091301 [[astro-ph/0208512](#)] [[INSPIRE](#)].
- [14] H. Jassal, J. Bagla and T. Padmanabhan, *WMAP constraints on low redshift evolution of dark energy*, *Mon. Not. Roy. Astron. Soc.* **356** (2005) L11 [[astro-ph/0404378](#)] [[INSPIRE](#)].
- [15] G. Efstathiou, *Constraining the equation of state of the universe from distant type Ia supernovae and Cosmic Microwave Background anisotropies*, *Mon. Not. Roy. Astron. Soc.* **310** (2000) 842 [[astro-ph/9904356](#)] [[INSPIRE](#)].
- [16] T.D. Saini, S. Raychaudhury, V. Sahni and A.A. Starobinsky, *Reconstructing the cosmic equation of state from supernova distances*, *Phys. Rev. Lett.* **85** (2000) 1162 [[astro-ph/9910231](#)] [[INSPIRE](#)];
U. Alam, V. Sahni, T.D. Saini and A. Starobinsky, *Exploring the expanding universe and dark energy using the statefinder diagnostic*, *Mon. Not. Roy. Astron. Soc.* **344** (2003) 1057

- [astro-ph/0303009] [INSPIRE]; *Is there supernova evidence for dark energy metamorphosis?*, *Mon. Not. Roy. Astron. Soc.* **354** (2004) 275 [astro-ph/0311364] [INSPIRE].
- [17] V. Sahni and A. Starobinsky, *Reconstructing dark energy*, *Int. J. Mod. Phys. D* **15** (2006) 2105 [astro-ph/0610026] [INSPIRE].
- [18] I. Maor, R. Brustein, J. McMahon and P.J. Steinhardt, *Measuring the equation of state of the universe: pitfalls and prospects*, *Phys. Rev. D* **65** (2002) 123003 [astro-ph/0112526] [INSPIRE];
 Y. Wang and P. Mukherjee, *Model-independent constraints on dark energy density from flux-averaging analysis of type-Ia supernova data*, *Astrophys. J.* **606** (2004) 654 [astro-ph/0312192] [INSPIRE];
 A. Upadhye, M. Ishak and P.J. Steinhardt, *Dynamical dark energy: current constraints and forecasts*, *Phys. Rev. D* **72** (2005) 063501 [astro-ph/0411803] [INSPIRE];
 Z.-K. Guo, N. Ohta and Y.-Z. Zhang, *Parametrization of quintessence and its potential*, *Phys. Rev. D* **72** (2005) 023504 [astro-ph/0505253] [INSPIRE];
 Y. Wang and P. Mukherjee, *Robust dark energy constraints from supernovae, galaxy clustering and three-year Wilkinson Microwave Anisotropy Probe observations*, *Astrophys. J.* **650** (2006) 1 [astro-ph/0604051] [INSPIRE];
 S. Nesseris and L. Perivolaropoulos, *A comparison of cosmological models using recent supernova data*, *Phys. Rev. D* **70** (2004) 043531 [astro-ph/0401556] [INSPIRE];
 R. Lazkoz, S. Nesseris and L. Perivolaropoulos, *Exploring cosmological expansion parametrizations with the gold SnIa dataset*, *JCAP* **11** (2005) 010 [astro-ph/0503230] [INSPIRE];
 S. Nesseris and L. Perivolaropoulos, *Tension and systematics in the Gold06 SnIa dataset*, *JCAP* **02** (2007) 025 [astro-ph/0612653] [INSPIRE];
 R. Crittenden, E. Majerotto and F. Piazza, *Measuring deviations from a cosmological constant: a field-space parameterization*, *Phys. Rev. Lett.* **98** (2007) 251301 [astro-ph/0702003] [INSPIRE];
 K. Ichikawa and T. Takahashi, *Dark energy parametrizations and the curvature of the universe*, *JCAP* **02** (2007) 001 [astro-ph/0612739] [INSPIRE];
 G.-B. Zhao, J.-Q. Xia, B. Feng and X. Zhang, *Probing dynamics of dark energy with supernova, galaxy clustering and the three-year Wilkinson Microwave Anisotropy Probe (WMAP) observations*, *Int. J. Mod. Phys. D* **16** (2007) 1229 [astro-ph/0603621] [INSPIRE];
 G.-B. Zhao et al., *Probing for dynamics of dark energy and curvature of universe with latest cosmological observations*, *Phys. Lett. B* **648** (2007) 8 [astro-ph/0612728] [INSPIRE].
- [19] WMAP collaboration, E. Komatsu et al., *Seven-year Wilkinson Microwave Anisotropy Probe (WMAP) observations: cosmological interpretation*, *Astrophys. J. Suppl.* **192** (2011) 18 [arXiv:1001.4538] [INSPIRE].
- [20] N. Suzuki et al., *The Hubble Space Telescope cluster supernova survey: V. Improving the dark energy constraints above $z > 1$ and building an early-type-hosted supernova sample*, *Astrophys. J.* **746** (2012) 85 [arXiv:1105.3470] [INSPIRE].
- [21] B.A. Bassett, M. Kunz, J. Silk and C. Ungarelli, *A late time transition in the cosmic dark energy?*, *Mon. Not. Roy. Astron. Soc.* **336** (2002) 1217 [astro-ph/0203383] [INSPIRE].
- [22] P.S. Corasaniti and E. Copeland, *A model independent approach to the dark energy equation of state*, *Phys. Rev. D* **67** (2003) 063521 [astro-ph/0205544] [INSPIRE].
- [23] T. Barreiro, E.J. Copeland and N. Nunes, *Quintessence arising from exponential potentials*, *Phys. Rev. D* **61** (2000) 127301 [astro-ph/9910214] [INSPIRE].
- [24] A. Albrecht and C. Skordis, *Phenomenology of a realistic accelerating universe using only Planck scale physics*, *Phys. Rev. Lett.* **84** (2000) 2076 [astro-ph/9908085] [INSPIRE];
 E.J. Copeland, N. Nunes and F. Rosati, *Quintessence models in supergravity*, *Phys. Rev. D* **62** (2000) 123503 [hep-ph/0005222] [INSPIRE].

- [25] B.A. Bassett, P.S. Corasaniti and M. Kunz, *The essence of quintessence and the cost of compression*, *Astrophys. J.* **617** (2004) L1 [[astro-ph/0407364](#)] [[INSPIRE](#)].
- [26] SUPERNOVA SEARCH TEAM collaboration, A.G. Riess et al., *Type Ia supernova discoveries at $z > 1$ from the Hubble Space Telescope: evidence for past deceleration and constraints on dark energy evolution*, *Astrophys. J.* **607** (2004) 665 [[astro-ph/0402512](#)] [[INSPIRE](#)].
- [27] WMAP collaboration, D. Spergel et al., *First year Wilkinson Microwave Anisotropy Probe (WMAP) observations: determination of cosmological parameters*, *Astrophys. J. Suppl.* **148** (2003) 175 [[astro-ph/0302209](#)] [[INSPIRE](#)].
- [28] R.J. Scherrer and A. Sen, *Thawing quintessence with a nearly flat potential*, *Phys. Rev. D* **77** (2008) 083515 [[arXiv:0712.3450](#)] [[INSPIRE](#)].
- [29] S. Dutta and R.J. Scherrer, *Hilltop quintessence*, *Phys. Rev. D* **78** (2008) 123525 [[arXiv:0809.4441](#)] [[INSPIRE](#)].
- [30] T. Chiba, *Slow-roll thawing quintessence*, *Phys. Rev. D* **79** (2009) 083517 [*Erratum ibid.* **D 80** (2009) 109902] [[arXiv:0902.4037](#)] [[INSPIRE](#)].
- [31] T. Chiba, S. Dutta and R.J. Scherrer, *Slow-roll k -essence*, *Phys. Rev. D* **80** (2009) 043517 [[arXiv:0906.0628](#)] [[INSPIRE](#)].
- [32] T. Chiba, *The equation of state of tracker fields*, *Phys. Rev. D* **81** (2010) 023515 [[arXiv:0909.4365](#)] [[INSPIRE](#)].
- [33] P.S. Corasaniti, M. Kunz, D. Parkinson, E. Copeland and B. Bassett, *The foundations of observing dark energy dynamics with the Wilkinson Microwave Anisotropy Probe*, *Phys. Rev. D* **70** (2004) 083006 [[astro-ph/0406608](#)] [[INSPIRE](#)].
- [34] E.V. Linder and D. Huterer, *How many dark energy parameters?*, *Phys. Rev. D* **72** (2005) 043509 [[astro-ph/0505330](#)] [[INSPIRE](#)].
- [35] J.A. Frieman, C.T. Hill, A. Stebbins and I. Waga, *Cosmology with ultralight pseudo Nambu-Goldstone bosons*, *Phys. Rev. Lett.* **75** (1995) 2077 [[astro-ph/9505060](#)] [[INSPIRE](#)].
- [36] R. Caldwell and E.V. Linder, *The limits of quintessence*, *Phys. Rev. Lett.* **95** (2005) 141301 [[astro-ph/0505494](#)] [[INSPIRE](#)].
- [37] W. Hu and I. Sawicki, *Models of $f(R)$ cosmic acceleration that evade solar-system tests*, *Phys. Rev. D* **76** (2007) 064004 [[arXiv:0705.1158](#)] [[INSPIRE](#)];
A.A. Starobinsky, *Disappearing cosmological constant in $f(R)$ gravity*, *JETP Lett.* **86** (2007) 157 [[arXiv:0706.2041](#)] [[INSPIRE](#)];
S.A. Appleby and R.A. Battye, *Do consistent $F(R)$ models mimic general relativity plus Λ ?*, *Phys. Lett. B* **654** (2007) 7 [[arXiv:0705.3199](#)] [[INSPIRE](#)];
S. Tsujikawa, *Observational signatures of $f(R)$ dark energy models that satisfy cosmological and local gravity constraints*, *Phys. Rev. D* **77** (2008) 023507 [[arXiv:0709.1391](#)] [[INSPIRE](#)];
H. Motohashi, A.A. Starobinsky and J. Yokoyama, *Phantom boundary crossing and anomalous growth index of fluctuations in viable $f(R)$ models of cosmic acceleration*, *Prog. Theor. Phys.* **123** (2010) 887 [[arXiv:1002.1141](#)] [[INSPIRE](#)].
- [38] M. Baldi, *Early massive clusters and the bouncing coupled dark energy*, *Mon. Not. Roy. Astron. Soc.* **420** (2012) 430 [[arXiv:1107.5049](#)] [[INSPIRE](#)].
- [39] V. Sahni, A. Shafieloo and A.A. Starobinsky, *Two new diagnostics of dark energy*, *Phys. Rev. D* **78** (2008) 103502 [[arXiv:0807.3548](#)] [[INSPIRE](#)].
- [40] E.E. Ishida, R.R. Reis, A.V. Toribio and I. Waga, *When did cosmic acceleration start? How fast was the transition?*, *Astropart. Phys.* **28** (2008) 547 [[arXiv:0706.0546](#)] [[INSPIRE](#)].
- [41] A.C.C. Guimaraes and J.A.S. Lima, *Could the cosmic acceleration be transient? A cosmographic evaluation*, *Class. Quant. Grav.* **28** (2011) 125026 [[arXiv:1005.2986](#)] [[INSPIRE](#)].

- [42] R. Giotri et al., *From cosmic deceleration to acceleration: new constraints from SN Ia and BAO/CMB*, *JCAP* **03** (2012) 027 [[arXiv:1203.3213](#)] [[INSPIRE](#)].
- [43] A. Shafieloo, V. Sahni and A.A. Starobinsky, *Is cosmic acceleration slowing down?*, *Phys. Rev. D* **80** (2009) 101301 [[arXiv:0903.5141](#)] [[INSPIRE](#)].
- [44] O.F. Piattella, D. Bertacca, M. Bruni and D. Pietrobon, *Unified dark matter models with fast transition*, *JCAP* **01** (2010) 014 [[arXiv:0911.2664](#)] [[INSPIRE](#)];
D. Bertacca, M. Bruni, O.F. Piattella and D. Pietrobon, *Unified dark matter scalar field models with fast transition*, *JCAP* **02** (2011) 018 [[arXiv:1011.6669](#)] [[INSPIRE](#)].
- [45] A.G. Riess et al., *A redetermination of the Hubble constant with the Hubble Space Telescope from a differential distance ladder*, *Astrophys. J.* **699** (2009) 539 [[arXiv:0905.0695](#)] [[INSPIRE](#)].
- [46] SDSS collaboration, W.J. Percival et al., *Baryon Acoustic Oscillations in the Sloan Digital Sky Survey data release 7 galaxy sample*, *Mon. Not. Roy. Astron. Soc.* **401** (2010) 2148 [[arXiv:0907.1660](#)] [[INSPIRE](#)].
- [47] J. Bond, G. Efstathiou and M. Tegmark, *Forecasting cosmic parameter errors from microwave background anisotropy experiments*, *Mon. Not. Roy. Astron. Soc.* **291** (1997) L33 [[astro-ph/9702100](#)] [[INSPIRE](#)];
Y. Wang and P. Mukherjee, *Observational constraints on dark energy and cosmic curvature*, *Phys. Rev. D* **76** (2007) 103533 [[astro-ph/0703780](#)] [[INSPIRE](#)].
- [48] W. Hu and N. Sugiyama, *Small scale cosmological perturbations: an analytic approach*, *Astrophys. J.* **471** (1996) 542 [[astro-ph/9510117](#)] [[INSPIRE](#)].
- [49] SDSS collaboration, D.J. Eisenstein et al., *Detection of the baryon acoustic peak in the large-scale correlation function of SDSS luminous red galaxies*, *Astrophys. J.* **633** (2005) 560 [[astro-ph/0501171](#)] [[INSPIRE](#)].
- [50] D.J. Eisenstein and W. Hu, *Baryonic features in the matter transfer function*, *Astrophys. J.* **496** (1998) 605 [[astro-ph/9709112](#)] [[INSPIRE](#)].
- [51] C. Blake et al., *The WiggleZ dark energy survey: testing the cosmological model with Baryon Acoustic Oscillations at $z = 0.6$* , *Mon. Not. Roy. Astron. Soc.* **415** (2011) 2892 [[arXiv:1105.2862](#)] [[INSPIRE](#)].
- [52] F. Beutler et al., *The 6dF galaxy survey: Baryon Acoustic Oscillations and the local Hubble constant*, *Mon. Not. Roy. Astron. Soc.* **416** (2011) 3017 [[arXiv:1106.3366](#)] [[INSPIRE](#)].
- [53] H. Akaike, *A new look at the statistical model identification*, *IEEE Trans. Automatic Control* **19** (1974) 716;
A.R. Liddle, *How many cosmological parameters?*, *Mon. Not. Roy. Astron. Soc.* **351** (2004) L49 [[astro-ph/0401198](#)] [[INSPIRE](#)].
- [54] V.H. Cardenas and M. Rivera, *The role of curvature in the slowing down acceleration scenario*, *Phys. Lett. B* **710** (2012) 251 [[arXiv:1203.0984](#)] [[INSPIRE](#)].